minerals

MDPI

Article

Supplementary Information for

Capacity of Chlorate to Oxidize Ferrous Iron: Implications for Iron Oxide Formation on Mars

Kaushik Mitra [1], Eleanor L Moreland [1] and Jeffrey G. Catalano [1, 2,*]

[1] Department of Earth & Planetary Sciences, Washington University, St. Louis, MO 63130, USA; k.mitra@wustl.edu
[2] McDonnell Center for the Space Sciences, Washington University, St. Louis, Mo 63130, USA.
* Correspondence: catalano@levee.wustl.edu

Received: date; Accepted: date; Published: date

Contents of the file:

Results
Table S1
Figure S1 to S7

Results

2.1 Chlorate-free Control Experiments

The chlorate-free control samples showed no evidence of Fe(II) oxidation during the duration of the kinetic experiment (Figure S1). The Fe(II) concentration and pH of the were monitored weekly and remain close to their respective starting concentrations in both pH 7 and 3 in chloride- and sulfate-rich environment (Figure S1). Similarly, the control experiment for the mineral precipitation studies in sealed serum-bottle reactors outside the anaerobic chamber did not show any significant decrease in [Fe(II)] and pH after a period of ~100 days (data not shown).

Table S1: Mineral proportions and coherent scattering domain sizes determined from Rietveld refinements.

Sample	Mineral 1	Mineral 2	Mineral 3	Mineral 4+	R_{wp}(%) ^{a}	R_{exp}(%) ^{a}	χ^2 ^{a}
C-6:1-10-pH7	Non-stoichiometric Magnetite 47±1% (49±1 nm) ^{b} Fe Occ. = 94±1 % ^{c} a = 8.3759±0.0003 Å ^{d}	Nano-goethite 29±2% (17±1 nm)	Lepidocrocite 15±1% (63±7 nm)	Hexahydrite 9±2% Halite 0.9±0.2%	10.4	9.2	1.3
C-6:1-100-pH7	Lepidocrocite 43±1%	Non-stoichiometric Magnetite 36.9±0.9% (37.8±0.5 nm) Fe Occ. = 93.6±0.7% a = 8.3781±0.0003 Å	Nano-goethite 20±2% (10.8±0.5 nm)	Halite 0.9±0.2%	10.4	8.6	1.5
C-10:1-10-pH7	Magnetite 48±2% (51.6±0.7 nm) Fe Occ. = 97.9±0.7% a = 8.3990±0.0003 Å	Green Rust 16±3%	Nano-goethite 36±3% (3.5±0.3 nm)		10.2	8.7	1.4
C-10:1-100-pH7	Magnetite 84±1% (43.3±0.3 nm) Fe Occ. = 99.5±0.3 % a = 8.3908±0.0002 Å	Nano-goethite 16±1% (15.6±0.8 nm)			10.6	9.2	1.2

S-6:1-5-pH7	Non-stoichiometric Magnetite 92.2±0.8% (35.7±0.2 nm) Fe Occ. = 94.6±0.3 % a = 8.3781±0.0003 Å	Goethite 7.8±0.8% (49±3 nm)		10.3	8.4	1.5
S-6:1-10-pH3	Nano-goethite 100% (6.4±0.2 nm)			8.4	7.7	1.2
S-6:1-10-pH7	Nano-goethite 100% (8.0±0.2 nm)			8.9	8.4	1.1
S-6:1-100-pH3	Schwertmannite 100%			8.1	8.0	1.0
S-6:1-100-pH7	Goethite 100%			10.1	9.3	1.2
S-10:1-10-pH3	Nano-goethite 100% (8.4±0.5 nm)			9.2	8.7	1.1
S-10:1-10-pH7	Magnetite 47±1% (92±1 nm) Fe Occ. = 100% a = 8.3963±0.0001 Å	Goethite 27.9±0.8%	Hexahydrite 25±1%	11.8	8.6	1.9

S-10:1-100-pH3	Schwertmannite 100%	7.4	7.4	1.0
S-10:1-100-pH7	Goethite 100%	9.0	7.5	1.5

[a] Statistical measures of the goodness of fit.

[b] Coherent scattering domain size.

[c] Fe occupancy in non-stoichiometric magnetite

[d] Unit cell parameter for magnetite

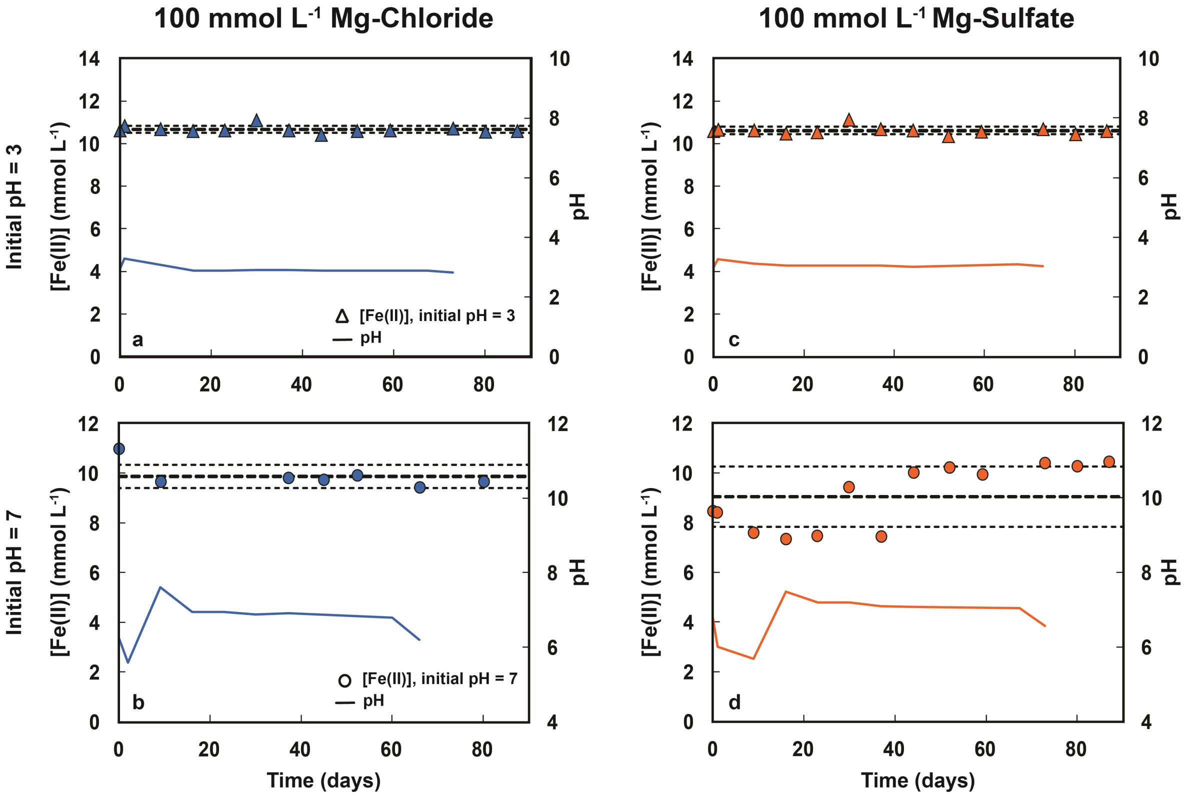

Figure S1: The dissolved Fe(II) concentration and pH versus time in systems containing approximately 10 mmol L^{-1} Fe(II) in 10^{-1} mol L^{-1} $MgCl_2$ at initial (a) pH 3 and (b) pH 7, and in 10^{-1} mol L^{-1} $MgSO_4$ fluids at initial (c) pH 3 and (d) pH 7 at 24°C. The thick dashed line corresponds to the average Fe(II) concentration in the experiment and the thin dashed lines correspond to ±1σ (standard deviation) of this concentration.

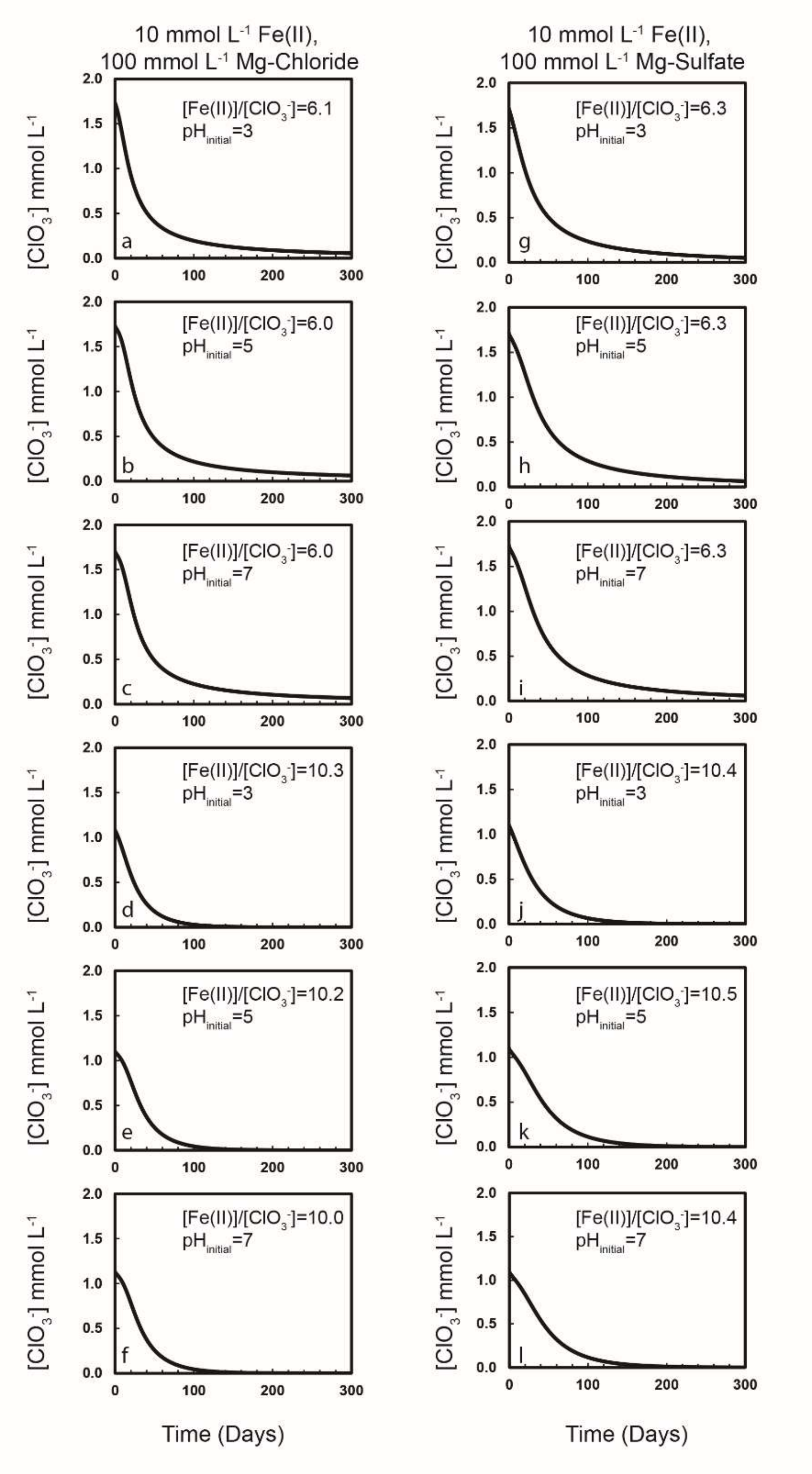

Figure S2: Simulated dissolved chlorate concentration versus time from the kinetic model for systems containing approximately 10 mmol L^{-1} Fe(II) in 0.1 mol L^{-1} $MgCl_2$ fluids (left column) and 0.1 mol L^{-1} $MgSO_4$ (right column) and 1.6 mmol L^{-1} ClO_3^- at initial pH 3 (a and g), pH 5 (b and h), and pH 7 (c and i), and 1.0 mmol L^{-1} ClO_3^- at initial pH 3 (d and j), pH 5 (e and k), and pH 7 (c and l) at 24°C.

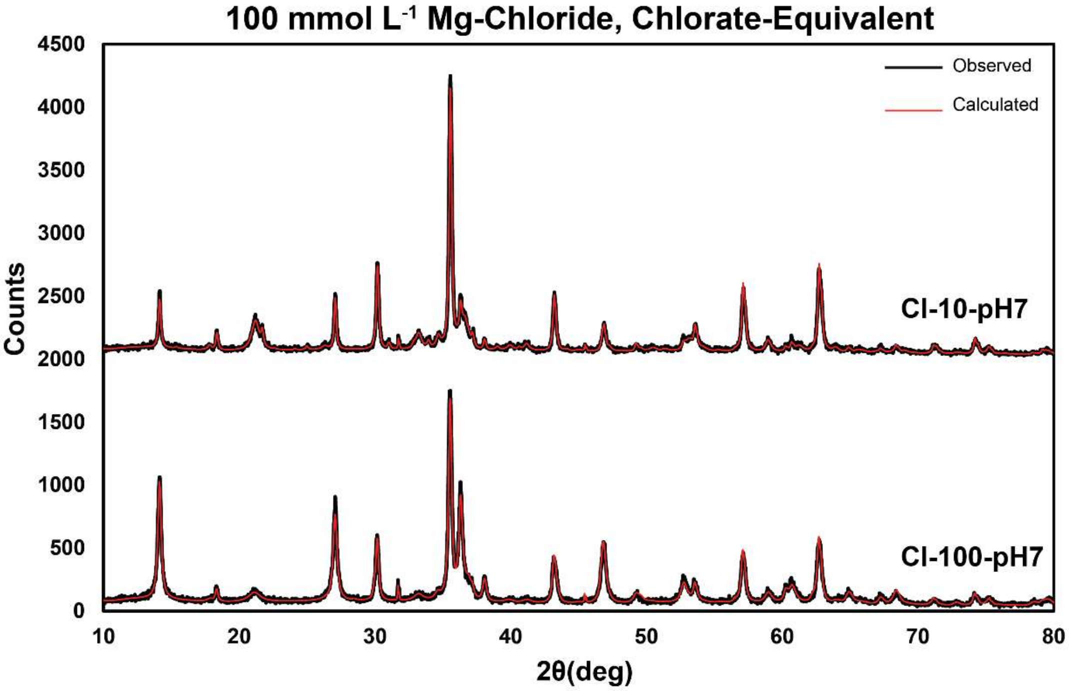

Figure S3: Rietveld refinements of the X-ray diffraction patterns for the solid-phase precipitates produced by Fe(II)-oxidation by chlorate in the chloride-rich, chlorate-equivalent solution by Fe(II) oxidation. The samples were abbreviated using the values of initial Fe(II) concentration in mmol L^{-1}, and initial pH (experimental details in Table 2 and S1).

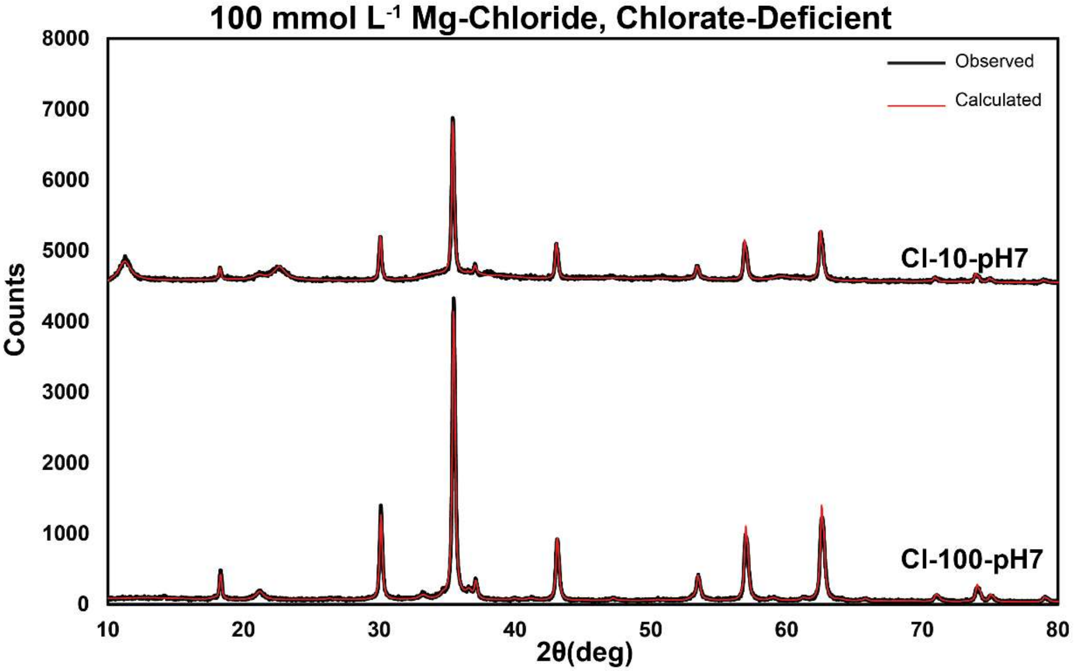

Figure S4: Rietveld refinements of the X-ray diffraction patterns for the solid-phase precipitates produced by Fe(II)-oxidation by chlorate in the chloride-rich, chlorate-deficient solution by Fe(II) oxidation. The samples were abbreviated using the values of initial Fe(II) concentration in mmol L^{-1}, and initial pH (experimental details in Table 2 and S1).

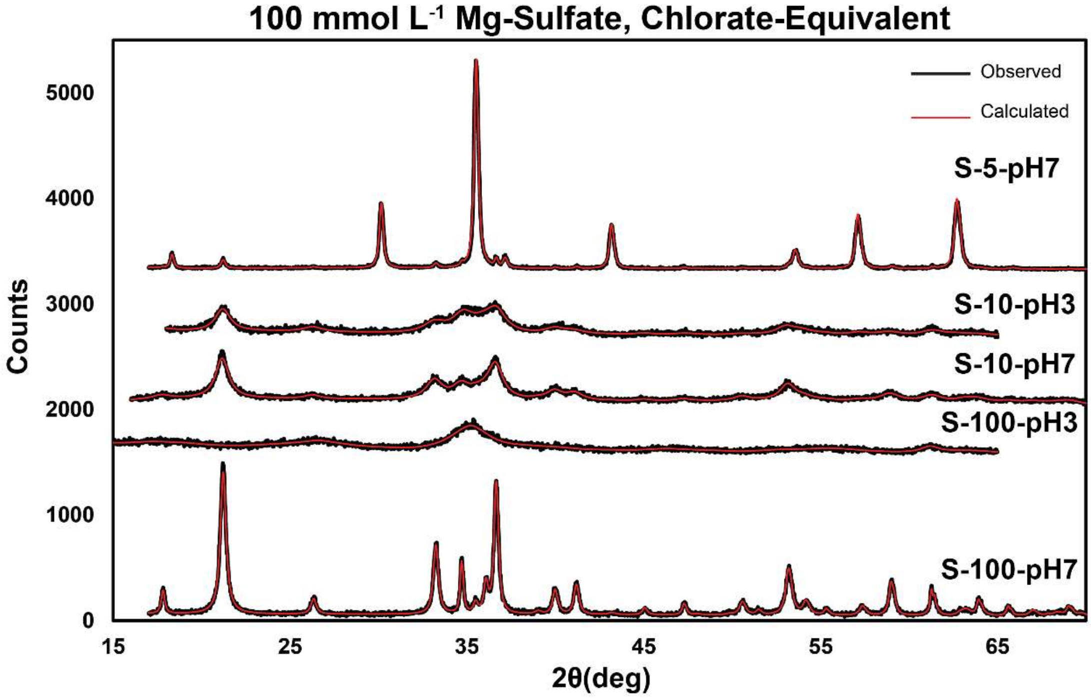

Figure S5: Rietveld refinements of the X-ray diffraction patterns for the solid-phase precipitates produced by Fe(II)-oxidation by chlorate in the sulfate-rich, chlorate-equivalent solution by Fe(II) oxidation. The samples were abbreviated using the values of initial Fe(II) concentration in mmol L-1, and initial pH (experimental details in Table 2 and S1).

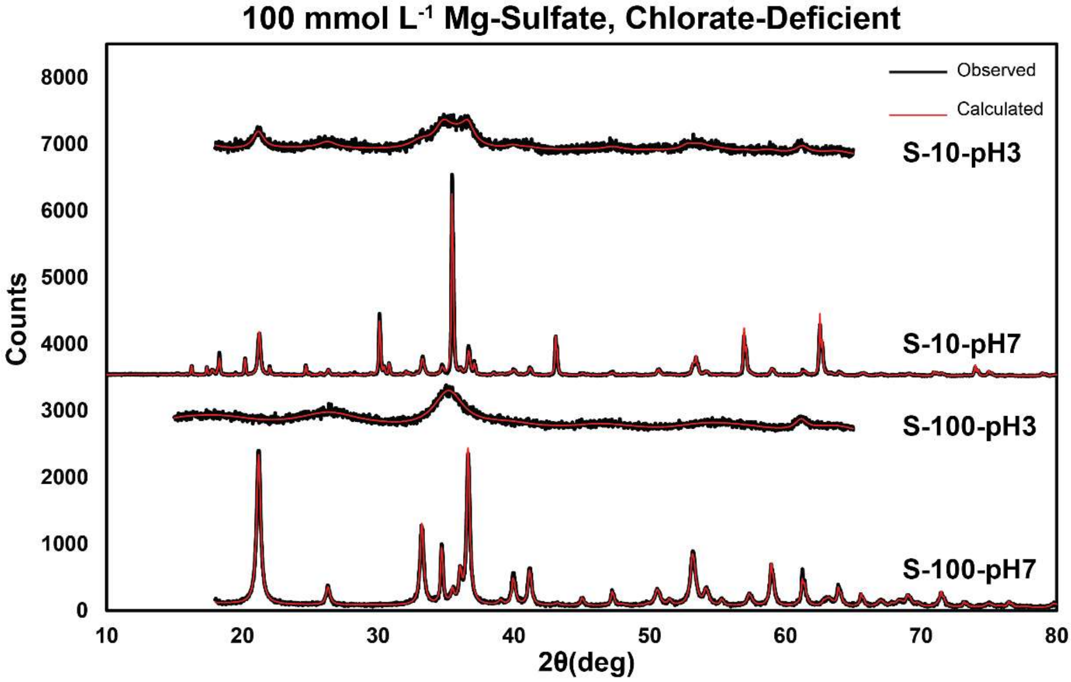

Figure S6: Rietveld refinements of the X-ray diffraction patterns for the solid-phase precipitates produced by Fe(II)-oxidation by chlorate in the sulfate-rich, chlorate-deficient solution by Fe(II) oxidation. The samples were abbreviated using the values of initial Fe(II) concentration in mmol L^{-1}, and initial pH (experimental details in Table 2 and S1).

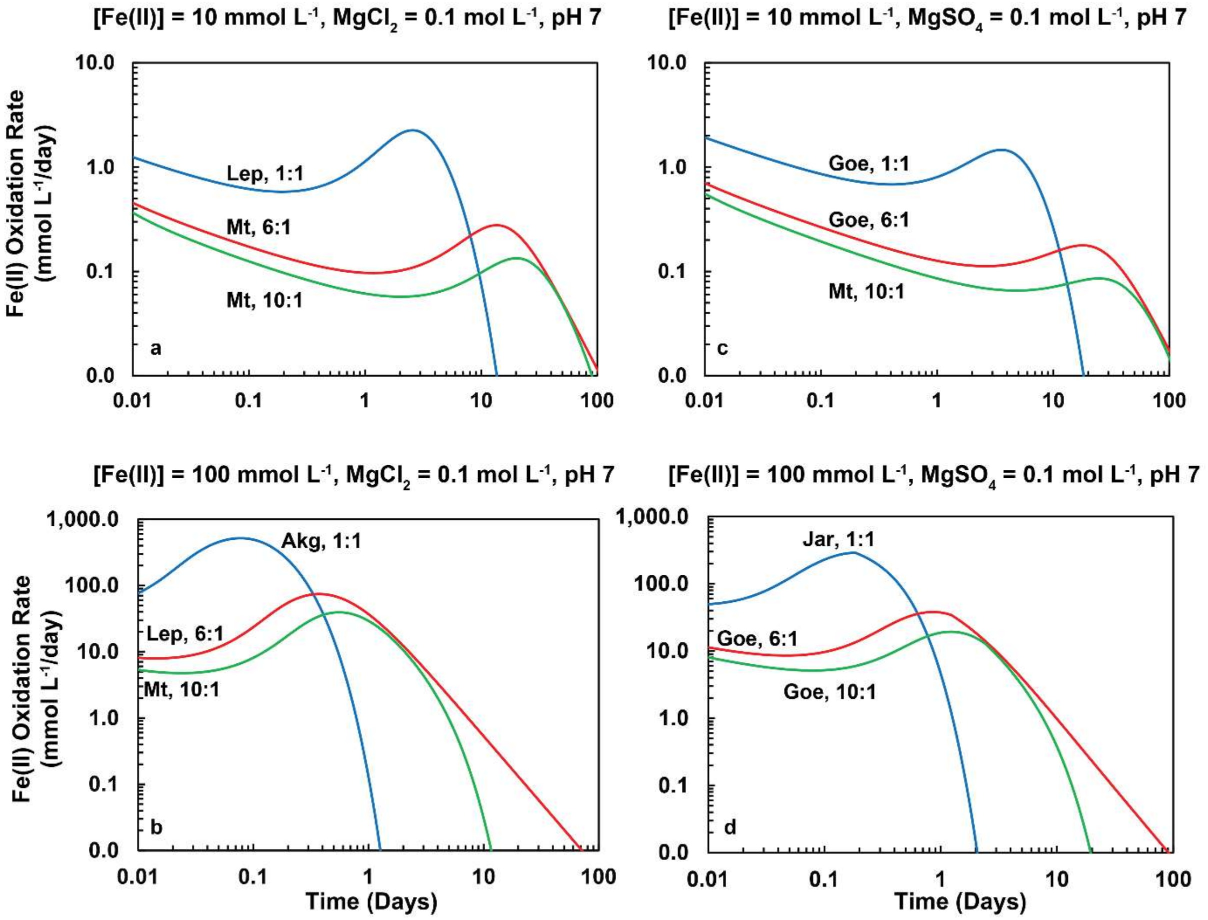

Figure S7: Simulated Fe(II) oxidation rate (mmol L^{-1} per day) versus time from the kinetic model with the corresponding dominant mineral produced in the mineral precipitation studies containing (a) 10 mmol L^{-1} Fe(II), 0.1 mol L^{-1} MgCl$_2$ at initial pH 7 and (b)) 0.1 mol L^{-1} Fe(II), 0.1 mol L^{-1} MgCl$_2$ at initial pH 7 (c) 10 mmol L^{-1} Fe(II), 10^{-1} mol L^{-1} MgSO$_4$ fluids at initial pH 7, and (d) 10 mmol L^{-1} Fe(II), 0.1 mol L^{-1} MgSO$_4$ fluids at initial pH 7 at 24°C. The ratio represented in the legend along the mineral name represent the molar ratio between [Fe(II)] and [ClO$_3^-$]. The mineral name codes are as: Mt =: Magnetite; Lep = Lepidocrocite; Akg = Akaganeite; Goe = Goethite; Jar = Jarosite.